Water Science & Technology

Spatiotemporal succession of phosphorous accumulating biofilms during the first year of establishment

Didrik Villard[a], Inger Andrea Nesbø Goa[b], Inga Leena Angell[b], Sondre Eikaas[c], Torgeir Saltnes[c,d], Wenche Johansen [iD][a] and Knut Rudi[a,b,*]

[a] Department of Biotechnology, Inland Norway University of Applied Sciences, Hamar, Norway
[b] Faculty of Chemistry, Biotechnology and Food Science, University of Life Sciences, Ås, Norway
[c] Hias, Ottestad, Hamar, Norway
[d] Hias How2O, Ottestad, Hamar, Norway
*Corresponding author. E-mail: knut.rudi@nmbu.no

[iD] WJ, 0000-0002-9240-586X

ABSTRACT

Many wastewater treatment plants are dependent on the utilization of microorganisms in biofilms. Our knowledge about the establishment of these biofilms is limited, particular with respect to biofilms involved in enhanced biological phosphorus removal (EBPR). These biofilms rely on polyphosphate-accumulating organisms (PAOs), requiring alternating oxic and anaerobic conditions for phosphorous uptake. This challenge has been solved using the Hias process, which combines moving-bed biofilm-reactor (MBBR) technology with physical transfer of biofilm-carriers from oxic to anaerobic zones. We combined biofilm fractionation with temporal analyses to unveil the establishment in the Hias process. A stable phosphorous removal efficiency of >95% was reached within 16 weeks of operation. Phosphorus removal, however, was not correlated with the establishment of known PAOs. The biofilms seemed associated with an outer microbiota layer with rapid turnover and an inner layer with a slow expansion. The inner layer showed an overrepresentation of known PAOs. In conclusion, our spatio-temporal analyses of phosphorous accumulating biofilm establishment lead to a new model for biofilm growth, while the mechanisms for phosphorous removal remain largely unresolved.

Key words: biofilm, ecology, 16S rRNA gene

HIGHLIGHTS

- New model for biofilm formation.
- Novel phosphorus removal process.
- Temporal analyses.
- Spatial analyses.
- New insight in microbial biofilm ecology.

GRAPHICAL ABSTRACT
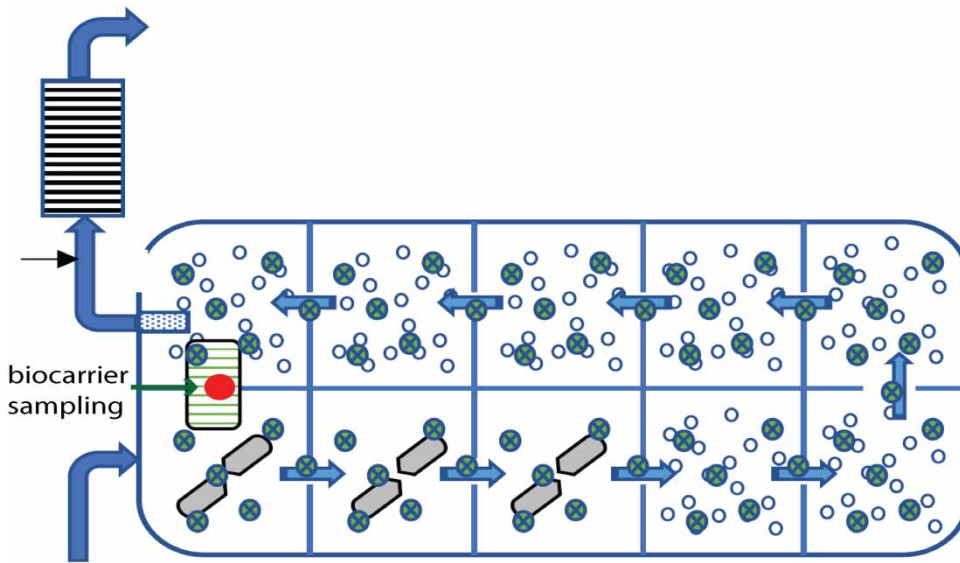
BACKGROUND

Biofilms are multifaceted, dynamic microbial communities composed of cells that are heterogeneous in space and time. Biofilm represents the main mode of microbial life and current estimates suggest that up to 80% of bacterial and archaeal organisms live in biofilms (Flemming & Wuertz 2019). Life in a biofilm provides competitive advantages to its microorganisms, including protection from environmental stressors and through cooperation between different cells to complement each other's metabolic requirements and biosynthetic pathways (Nadell *et al.* 2016). Fundamental to the survival of microorganisms in their environment is energy generation, where the availability of nutrients dictates metabolic activity and hence the function of the microorganism and biofilm. For environmental microorganisms, energy generation is generally highly dependent on shifting gradients of electron donors and/or acceptors (Falkowski *et al.* 2008). In biofilms, shifting gradients are created through microbial activity, solute diffusion rates, and biofilm geometry, resulting in the spatial distribution of nutrients through cell biomass and the extracellular matrix (Flemming *et al.* 2016).

Biofilms can be composed of more than one thousand bacterial species (Angell *et al.* 2017) and recent evidence suggests that the microbial composition of mature biofilms can be stable for years (Angell *et al.* 2020). The spatiotemporal successions and the establishment of mature biofilms, however, remain mainly unresolved (Nadell *et al.* 2016). Particularly intriguing is the understanding of the establishment of biofilms that require fluctuating environments for proper and stable functioning. In this respect, and of particular interest are biofilm communities capable of accumulating and removing phosphorus from wastewater by the process of enhanced biological phosphorus removal (EBPR). Wastewater treatment processes based on EBPR rely on polyphosphate-accumulating organisms (PAOs), a group of bacteria performing alternating anaerobic and aerobic energy generation processes resulting in luxurious phosphorus uptake and intracellular storage as polyphosphate, poly-P. During anaerobic conditions, PAOs use stored poly-P as an energy reservoir to assimilate volatile fatty acids (VFAs) and store these as polyhydroxyalkanoates (PHA) intracellularly. When the PAOs are subjected to oxic conditions, PHA is used as an electron donor and carbon source to generate energy for maintenance and biomass growth and to restore the intracellular poly-P pool. The Hias process is a novel wastewater treatment technology based on the principles of EBPR combined with moving-bed biofilm-reactor (MBBR) technology developed at Hias IKS in Ottestad, Norway (Saltnes *et al.* 2017), using Kaldnes K3 biofilm-carriers as biomedium. After an initial filtration, the wastewater is introduced into the Hias reactor (Figure 1). The reactor is divided into ten reactor zones, the first three being anaerobic and the last seven being oxic, fulfilling the PAO's requirement for alternating conditions. In the tenth zone, the biofilm-carriers are lifted back to the first reactor zone using a conveyor belt, eliminating the need to recycle sludge for inoculation, as is common in active sludge methods of EBPR. The effluent wastewater from the tenth zone is sent to a sedimentation tank where extracted phosphorus can be precipitated and retrieved. The whole process takes approximately 8 h. The Hias process is

Hias plant

biocarrier
sampling
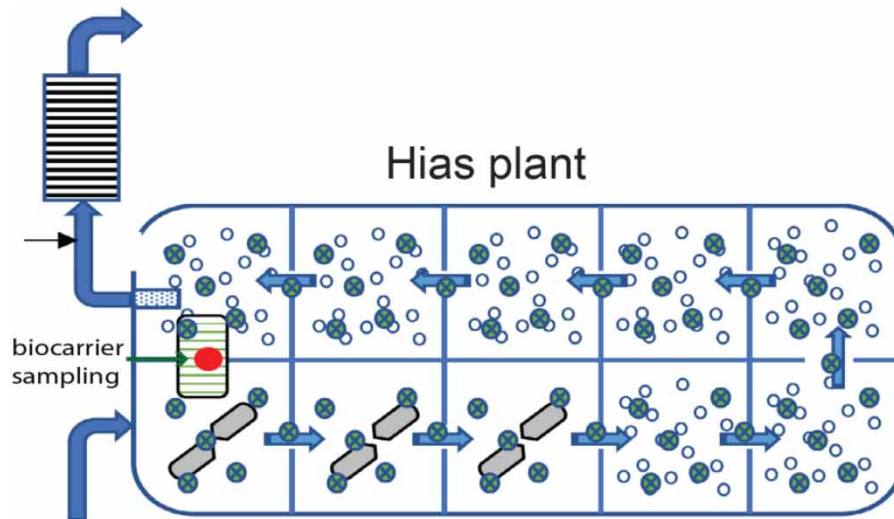
Weekly sampling from June 2016 to September 2017
- approx 10 biocarriers per sampling
  • stored at -20°C
- measurements of operational parameters
  • temperature celsius
  • load gPO4/m2d
  • % PO4 removed
  • % SCOD removed anaerobically
  • SCOD load: gSCOD/m2day
  • SCOD removed g/m2day
  • Q (m3/t)

three biocarriers per week
- • extraction of total DNA

three biocarriers per month
- • fractionation by mechanical treatment
- • extraction of total DNA from each fraction

all DNA extracts
- • qPCR targeting the 16S rRNA gene
- • Amplicon sequencing of the 16S rRNA gene
- • Taxonomic assignment using Siva
- • Functional assignment using MIDAS

Figure 1 | Outline of the analytical strategy. Sampling of biofilm-carrier was done on the conveyor belt, while the chemical measurements were done at both the inlet and the outlet.

implemented in a full-scale wastewater treatment plant at Hias IKS in Ottestad, Norway, with a capacity of 140,000 person equivalents (PE). The Waste Water Treatment Plant (WWTP) is the recipient of municipal wastewater from four municipalities in Norway (Hamar, Løten, Ringaker, and Stange) and the terminal recipient of the processed wastewater is Norway's largest lake, Mjøsa. This reactor is the study subject for the current study. The Hias process has proven highly stable in the long term and delivers a phosphorus removal efficiency above 95% (Saltnes *et al.* 2017). Previously, we have characterized

the mature Hias biofilm showing the functional stratifications of individual biofilm layers (Rudi *et al.* 2019; Villard *et al.* 2022). However, knowledge of how this highly effective phosphorus-accumulating biofilm, which is formed naturally without external inoculations, is established is still lacking.

The aim of this work was therefore to investigate the spatiotemporal development of the Hias biofilm during the first year of establishment. We analyzed biofilm samples from the startup operation of the first full-scale plant worldwide utilizing the Hias process.

MATERIALS AND METHODS

An outline of the experimental approach is provided in Figure 1.

Wastewater and reactor configuration

The inlet municipal wastewater has a continuous, unregulated, flow that varied in volume between 56.4 and 144 m³/t, with higher volumes causing increased flow rate, and lower causing a decrease. Retention time in the anaerobic reactor zones is set to constitute 30% of the full cycle regardless of inlet volume. In oxic reactor zones, dissolved oxygen (DO) levels are monitored for automatic dosing of air to maintain removal rates. The temperature fluctuated from 6.76 to 14.77 °C during the study period.

Chemical measurements

The wastewater in the Hias process plant was analyzed in parallel with biofilm-carriers for correlation with the biofilm microbiota composition. The samples for chemical analyses were filtered through 1.2 μm fiberglass filter and analyzed for dissolved phosphate and Soluble Chemical Oxygen Demand (SCOD) with a NOVA spectroquant 60 spectrometer (Merck).

Sampling of biofilms

The Hias reactor was started 2016-06-27, with biofilm-carriers being collected approximately once a week from 2016-06-03 to 2017-09-06, and immediately stored at −20 °C before further processing. The material collection took place at the end of the aerobic zones (outlined in Figure 1).

Fractionation and DNA extraction

Fractionation of the biofilm in three fractions, representing the outer, the middle, and the inner layer of the biofilm was performed as previously described (Villard *et al.* 2022).

For DNA extraction, the samples were mechanically disrupted 2×40 s in FastPrep96 (MP Biomedicals, USA) at 1,800 rpm with 5 min break between the runs. DNA was isolated by the KingFisher flex robot (Thermo Fisher Scientific, USA) using the MagMidi LGC kit (LGC genomics, UK) with 50 μL lysate, as previously described (Angell *et al.* 2017).

Quantitative PCR

The 16S rDNA gene copy number in biofilms, both intact and fractionated samples, was quantified using quantitative polymerase chain reaction (qPCR). qPCR was performed in a 25 μL volume using 2 μL DNA in a $1 \times$ HOT FIREPol® EvaGreen® qPCR supermix (Solis BioDyne, Estonia) with 0.2 μM of each the forward primer, Uni 341F, and the reverse primer Uni 806R (Angell *et al.* 2017). The reaction mix was then amplified and quantified by a LightCycler480 II (Roche, Germany) on the following program 95 °C for 15 min (95 °C for 30 s, 55 °C for 30 s, and 72 °C for 45 s) $\times 40$.

Illumina sequencing

The sequencing was done as previously described (Angell *et al.* 2017). The sequences went through pre-processing which involved, demultiplexing, truncating primers and quality filtering using QIIME (Caporaso *et al.* 2010). The following step involved processing using USEARCH v8 (Edgar 2010), where the OTUs were first clustered at a 97% homology level creating an OTU-table, and then the OTUs taxonomically assigned using the SILVA database (Quast *et al.* 2013). The composition of functional bacteria was determined by comparing the EBPR and MiDAS databases, with functions being assigned based on taxonomic matches to the OTUs.

Data analyses

Basic statistical analyses were done using MINITAB 18 (MINITAB Inc). Multivariate and ecological analyses were done in the Matlab programming environment, with PLS Toolbox (Eigenvector Inc) for multivariate analyses and the Fathom toolbox for ecological analyses (www.marine.usf.edu/user/djones/matlab/matlab.html).

Data deposition

Raw reads from the prokaryote and eukaryote SSU gene sequencing are available in the Sequence Read Archive (SRA) database with the accession number PRJNA513239.

RESULTS

The middle layer of the biofilm shows the most stable 16S rRNA gene copy number throughout the biofilm maturation process

The total number of 16S rRNA gene copies per biofilm sample was estimated to range from 10^6 to 10^9 through the experimental period of 56 weeks (Figure 2). Surprisingly, biofilm material harvested at the earliest time point after process startup (week 1), contained the highest 16S rRNA gene copy number, 10^9, with a gradual decrease to approximately 10^6 copies in week 27. After week 27, an increase and subsequent stabilization of the 16S rRNA gene copy number to approximately 10^8 was observed. Of the three spatial biofilm fractions, the middle layer (fraction 2) showed a relatively stable 16S rRNA gene copy number of 10^7 throughout the experimental period, while the copy numbers for the innermost (fraction 3) and the outer layer (fraction 1) showed larger fluctuations in numbers (Figure 2).

Maximum EBPR performance is established quickly and is not correlated to an increase in known PAOs

EBPR-process performance throughout the experimental period of 56 weeks was investigated by analyzing phosphorus and SCOD removal efficiencies based on the corresponding concentrations in the inlet (SCOD: 97–736 (mg/L); PO_4: 0.9–11.4 (mg/L)) and effluent (SCOD: 66–221 (mg/L); PO_4: 0.027–4.38 (mg/L)) wastewater streams, the C/P ratio being stable throughout the studied period, ranging from 54.5 to 83.7. A stable phosphorous removal efficiency of >95% was reached within 16 weeks of operation, while anaerobic SCOD removal lagged slightly behind, reaching its maximum of approximately
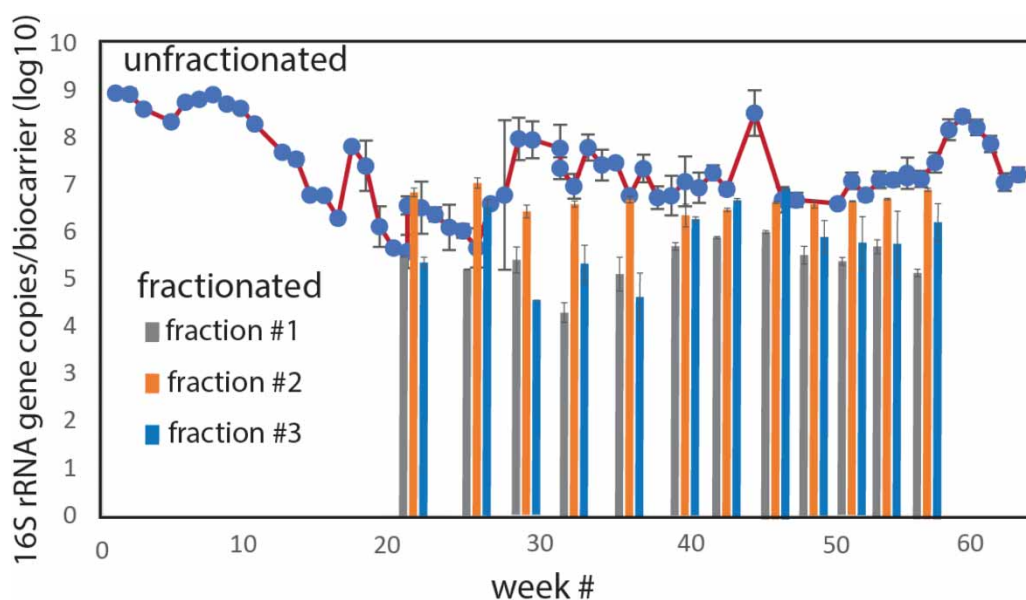

Figure 2 | Quantification of 16S rRNA gene copy numbers per biofilm-carrier. Gene copy numbers were quantified both for the unfractionated and the fractionated biofilm. The unfractionated biofilm (line plot), while the fractionated biofilm (bar plot) was analyzed from week 23 to 56. Mean values and standard deviations are shown for each analytical point. The analytical point with only a single measurement are represented without standard deviation.

60% after 6 months of operation (Figure 3(a)). Thus, the biofilm continued to increase SCOD removal efficiency, even though phosphorus removal efficiency was at its maximum. Details are shown in Supplementary Table S2.

The MiDAS database (McIlroy *et al.* 2017) was used to link the identity of abundant microorganisms in unfractionated biofilm samples to their functional importance. Based on functional group assignments, we identify an overall gradual increase in the number of PAOs, reaching a maximum of around 7% by the end of week 57 (Figure 3(b)). This increase in PAOs was not correlated to the observed major increase in phosphorus removal efficiency at approximately 16 weeks of operation. The increase in PAOs was associated with an increase in *Tetrasphaera* (Supplementary Table S1), which is one of the most common PAOs in EBPR-based wastewater treatment plants (Marques *et al.* 2017). In contrast to PAOs, glycogen-accumulating organisms (GAOs) were stably present at low levels (approximately 1%) throughout the whole experimental period. The numbers of bacteria capable of fermentation were also stable throughout the experimental period, with *Clostridium* as the most abundant genus. Denitrifies showed major fluctuations from week 1 to 57, being dominated by *Acidovorax* (Figure 3(b), Supplementary Table S1), while the level of nitrifiers was very low throughout the whole experimental period, ranging between 0.01 and 0.15%.

The functional composition of the individual Hias biofilm fractions remained relatively stable throughout the whole period analyzed (until week 40) (Figure 4). PAO abundancy increased toward the innermost part of the biofilm (fraction 3), while denitrifies were most abundant in the outermost layers (fractions 1 and 2). Fermenters, on the other hand, was most abundant in the middle layer (fraction 2) of the biofilm (Figure 4).
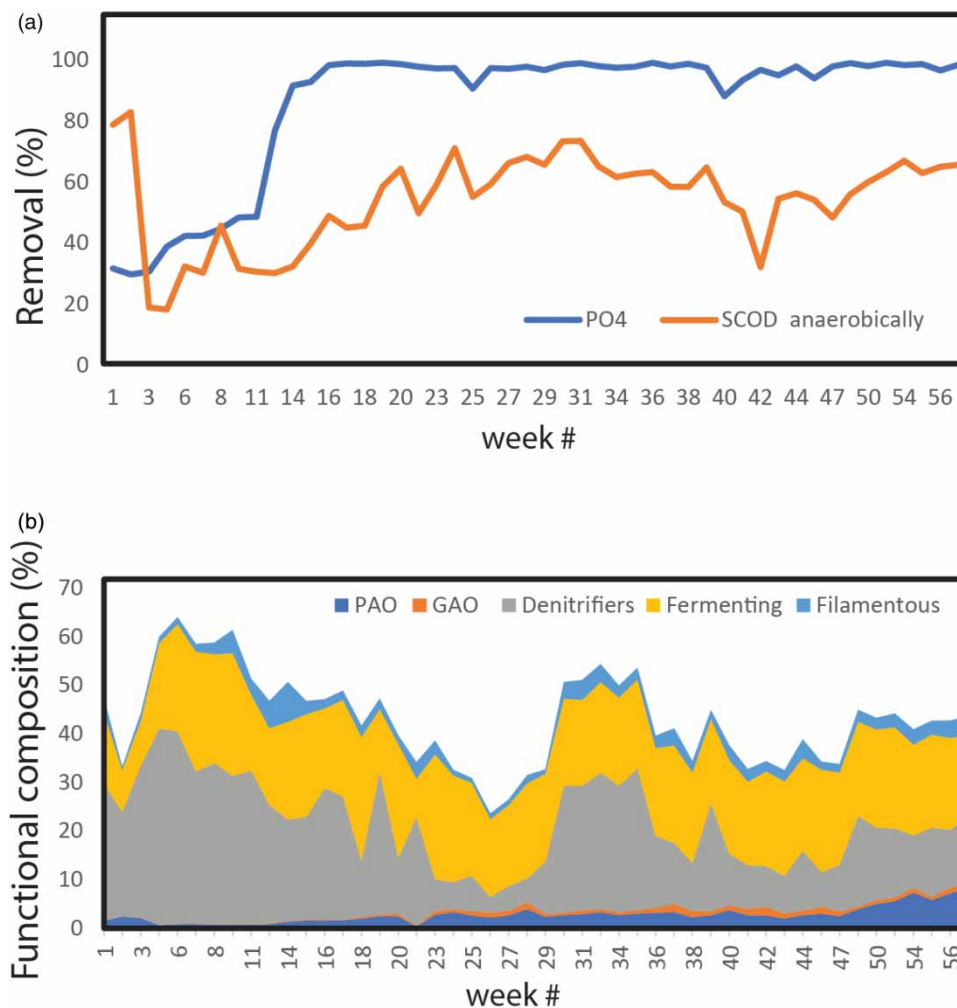

Figure 3 | Chemical removal (a) and functional profile of the biofilm (b). (a) The percental phosphorous removal (PO$_4$) and organic carbon (SCOD) during the experimental period. (b) The functional profile of the biofilm was based on properties derived from the MiDAS database.
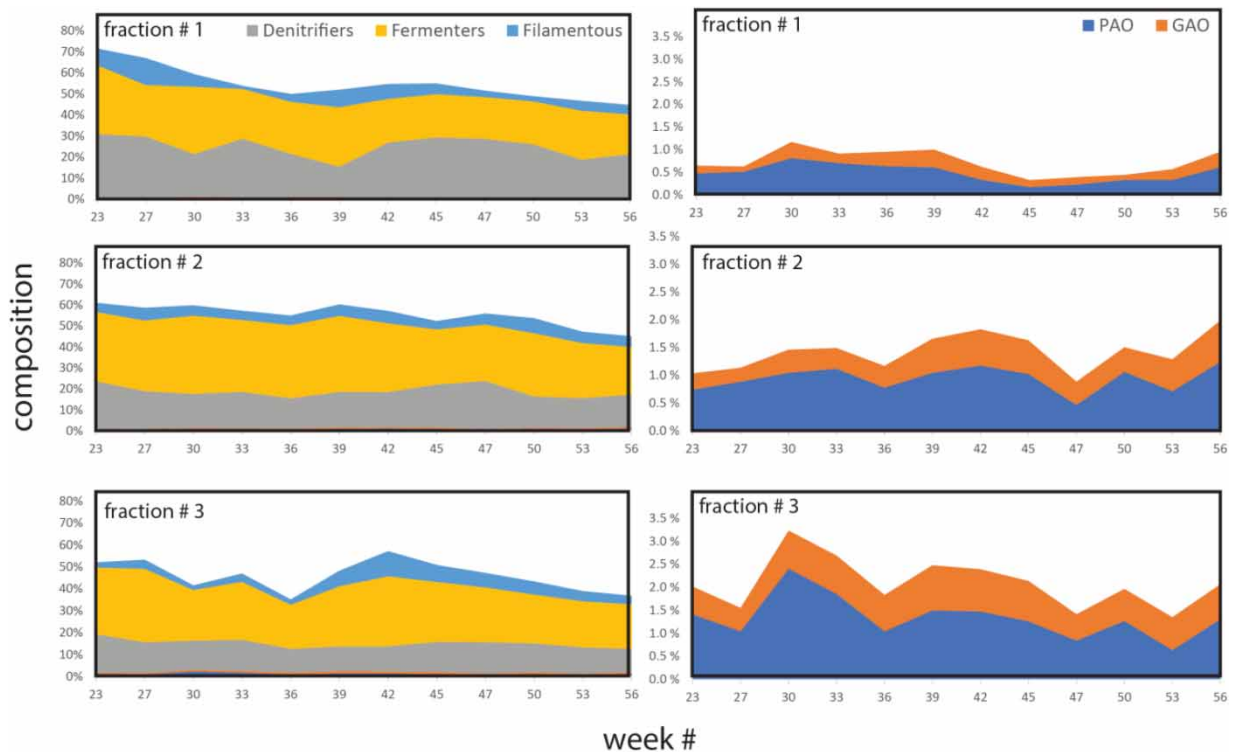
Figure 4 | Functional profile of the biofilm by fraction. Separate plots were made for PAOs and GAOs, because these represent minor portions of the microbiota. The functional profile of the biofilm was derived based on properties derived from the MiDAS database.

Initial colonizers were associated with the outer part of the biofilm, while succession was associated with predation

The overall taxonomic succession in microbiota composition throughout the experimental period of 56 weeks was determined by multivariate curve resolution (MCR) analysis to identify independent co-occurring components of the microbiota (de Juan & Tauler 2021). MCR analysis revealed four main components (Figure 5(a)). As visualized from the loading plot, the first component was mainly associated with the predatory genus *Peridibacter* (OTU 308) within the family *Bacteriovoracaceaea*. The second component was mainly associated with an uncharacterized bacterium OTU 56 within the *Bradyrhizobiaceae* family, in addition to OTU 24 representing uncultured *Desulfovibrio* species. Component 3 was mainly represented by OTU 146, an uncultured *Novosphingobium* species, with a minor component consisting of the genus *Aminobacter* (OTU 154). Finally, component 4 showed a dominance of the genus *Achromobacter* (OTU 9) (Figure 5(a)). Component 4 dominated initially, from week 1 to week 4, and was replaced by component 2. Components 1 and 2 alternated from week 25 to week 35, while component 3 appeared and increased rapidly at the end of the first year of establishment (Figure 5(a)).

We finally investigated the distribution of the signature genera for the MCR components for the fractionated biofilms. *Achromobacter*, which is a signature for MCR component 4 dominated the outer portion of the biofilm, while *Novosphingum* (signature for component 3) was most abundant in the inner part. The predatory *Peridibacter*, the indicator for component 1, seemed to be most abundant in the middle layer, while the anaerobic sulfur-reducing *Desulfovibrio*, being the indicator of MCR component 2, also seemed overrepresented toward the innermost part of the biofilm (Figure 5(b)).

DISCUSSION

The Hias biofilm is established with microorganisms naturally inhabiting sewage wastewater streams without intentional inoculations in an open system with a continuous inflow of new colonizers (Rudi *et al.* 2019). Therefore, the current five-step model (Sauer *et al.* 2022) is expected to have limited value for understanding how the surface-based complex biofilm in the Hias process is established. Our current analyses of the Hias biofilm suggest that initial colonizers were localized to the outermost fraction, representing the biofilm-water interface, while late colonizers were in deeper layers of the biofilm
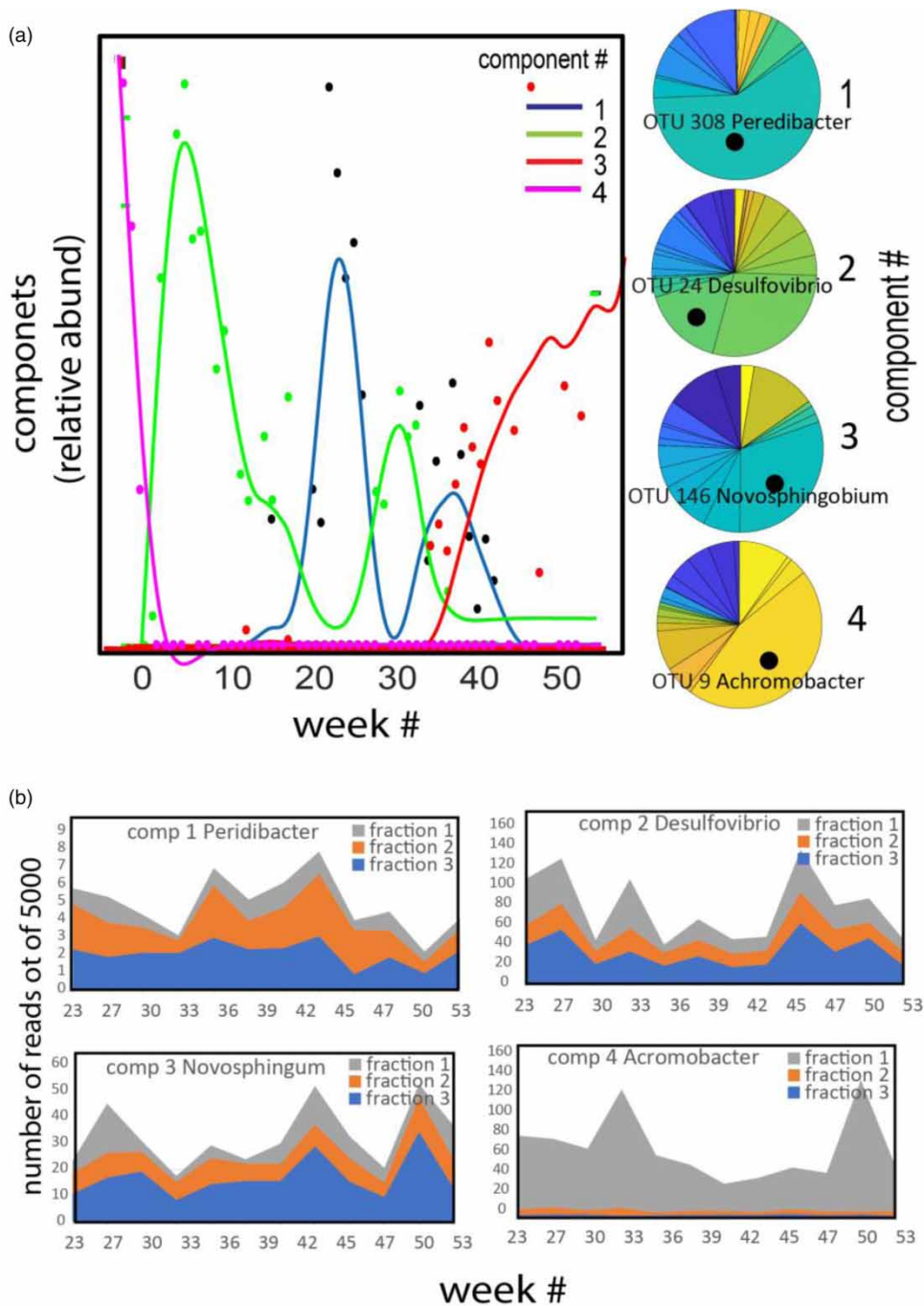
Figure 5 | Identification of main microbiota components by multivariate curve resolution (a) and spatiotemporal distribution of signature taxa (b). We identified four main components. Component 1 explained 27.7% of the variance, component 2 explained 10.7%, component 3 explained 3.9%, and component 4 explained 16.2%. The loadings indicate the genera that are important for the different MCR components. (b) The spatiotemporal distribution of the genera that are characteristic for the different MCR components are shown.

toward the wall of the biofilm-carrier. This pattern supports a microbiota establishment with a slow succession for the deepest layers of the biofilm, while the microbiota at the biofilm surface is characterized by rapid initial establishment and turnover. This result is not unexpected since microorganisms buried deep inside a biofilm are more protected from the environmental impact on the surface, and the microbiota could therefore gradually develop and adapt to their environment while protected from the potentially unfavorable conditions on the surface by the outer layer/initial colonizers. On the surface, however, the

microorganisms are highly exposed to stressors and changes in the environment, forcing the rapid establishment and turnover of the microbiota. The stability of the middle layer, on the other hand, could potentially be explained that this layer is in an equilibrium state.

We identified an abrupt increase in the phosphorus removal efficiency, from 30 to 95%, after approximately 12 weeks of process operation, which interestingly was not correlated to a corresponding increase in the abundance of known PAOs. This may indicate the proliferation of unknown phosphorus-accumulating microorganisms that are yet to be characterized (Hiraishi et al. 1991; Wang et al. 2018). Alternatively, the PAOs present exhibit a much higher potential for phosphorus accumulation, which possibly because of more favorable conditions was increased resulting in a sudden and high increase in the phosphorus removal efficiency later in the establishment of the process. The delayed increase in PAO population compared to phosphorus removal could be caused by the PAOs depending on acquiring poly-P storages in order to accumulate PHA as a carbon source. Studies on induced starvation in PAOs have shown that when endogenous polymer stores are depleted phosphorus removal is significantly hampered (Sun et al. 2022) and slower uptake of VFAs when recovering from depletion (Vargas et al. 2013). This suggests that accumulation of phosphorus could be a prerequisite for increase in PAO population, thus it would be expected to see phosphate removal increase prior to PAO population. The increase in phosphorus removal efficiency coincided, however, with a major increase in predatory bacteria belonging to the genus *Peridibacter* (Rotem et al. 2014). This result suggests that predation could play an important role in the shaping of the phosphorus-accumulating abilities of the Hias biofilm. The predation pressure has been suggested to be an important factor regulating the abundance of aerobic and anaerobic ammonium oxidizing bacteria in biofilms used for nitrogen removal from wastewater (Suarez et al. 2015). Changes in fermenters, providing VFAs and other substances that favor unknown PAOs, prior to the increase in P removal could also potentially, partially explain the early onset P removal. Given that the process extracts P for fertilizer from polyphosphates in PAOs that are found in the effluent wastewater, a certain amount of PAOs are dispersed from the biofilms into the wastewater. It is possible that this mechanism is related to shedding of PAOs in the outer layer suggesting that the lower abundance of PAOs in the outer layer is crucial to the removal of phosphorus in the Hias process, however further studies are needed on the dispersal of the Hias biofilm to say for certain.

Given that 95% P removal is reached prior to peak anaerobic SCOD removal of 60%, the anaerobic retention time is more than sufficient to favor carbon storage in PAOs. This is not surprising as a study on a lab-scale sequencing batch reactor-EBPR reactor has found that C/P ratio of 35 to optimize system stability for phosphorus removal, while higher ratios divert excess carbon to GAOs (Majed & Gu 2019). This is, however, mirrored in the consistently low abundance found in the current study. A potential explanation for the low GAO abundance could be related to water temperature, as higher water temperatures (>30 °C) favor GAOs, whereas lower temperatures, like observed during the study period, are known to favor PAOs (Law et al. 2016). Low GAO populations despite high C/P ratio opens the door to facilitate denitrification, as this process also requires organic carbon, if the Hias process are to be implemented in locations where nitrogen removal requirements apply, while still maintaining a stable phosphorus removal. The very low levels of nitrifiers could be explained by the low temperature and relatively low retention time in the reactors, but this needs to be investigated further.

We have recently shown functional stratification of mature Hias biofilm, with nitrate assimilation at the surface layer, fermenters in the middle layer, and PAOs in the innermost layer (Villard et al. 2022). Similar functional patterns were observed in the current study, for the establishment of the Hias biofilm. However, although the PAOs showed the highest relative level in the deepest layer of the biofilm, the overall abundance level of PAOs was low, <5% until week 47, with a slight increase from week 47 to 57 of operation. This indicates a very slow accumulation in the biofilm of microorganisms established to have known PAO properties.

Taken together, the spatiotemporal analyses of Hias biofilm establishment unveiled novel patterns with respect to how both the composition and function of a biofilm in an open system are established and opened new questions related to the efficiency of the phosphorous accumulating abilities of the PAOs in a phosphorus-accumulating biofilm.

CONCLUSION

In conclusion, during the establishment of the Hias biofilm, phosphorus removal was found to rapidly increase prior to any observed increase in known PAOs. The microbiota of the biofilm showed a slow succession of colonization with the first settlers associated with the outer layer of the biofilm in direct contact with the wastewater, and later colonizers accumulating on

the inner layers of the biofilm. Even with >95% phosphorus removal by week 16, known PAOs continue to increase in abundance throughout the 57 weeks studied.

ACKNOWLEDGEMENTS

DATA AVAILABILITY STATEMENT

All relevant data are included in the paper or its Supplementary Information.

CONFLICT OF INTEREST

The authors declare there is no conflict.

REFERENCES

Angell, I. L., Hanssen, J. F. & Rudi, K. 2017 Prokaryote species richness is positively correlated with eukaryote abundance in wastewater treatment biofilms. *Lett. Appl. Microbiol.* **65**, 66–72.

Angell, I. L., Bergaust, L., Hanssen, J. F., Aasen, E. M. & Rudi, K. 2020 Ecological processes affecting long-term eukaryote and prokaryote biofilm persistence in nitrogen removal from sewage. *Genes (Basel)* **11**, 1–14.

Caporaso, J. G., Kuczynski, J., Stombaugh, J., Bittinger, K., Bushman, F. D., Costello, E. K., Fierer, N., Pena, A. G., Goodrich, J. K., Gordon, J. I., Huttley, G. A., Kelley, S. T., Knights, D., Koenig, J. E., Ley, R. E., Lozupone, C. A., McDonald, D., Muegge, B. D., Pirrung, M., Reeder, J., Sevinsky, J. R., Turnbaugh, P. J., Walters, W. A., Widmann, J., Yatsunenko, T., Zaneveld, J. & Knight, R. 2010 QIIME allows analysis of high-throughput community sequencing data. *Nat. Methods* **7**, 335–336.

de Juan, A. & Tauler, R. 2021 Multivariate curve resolution: 50 years addressing the mixture analysis problem – a review. *Anal. Chim. Acta* **1145**, 59–78.

Edgar, R. C. 2010 Search and clustering orders of magnitude faster than BLAST. *Bioinformatics* **26**, 2460–2461.

Falkowski, P. G., Fenchel, T. & Delong, E. F. 2008 The microbial engines that drive Earth's biogeochemical cycles. *Science* **320**, 1034–1039.

Flemming H.-C. & Wuertz S. 2019 Bacteria and archaea on Earth and their abundance in biofilms. *Nature Reviews Microbiology* **17** (4), 247–260.

Flemming, H.-C., Wingender, J., Szewzyk, U., Steinberg, P., Rice, S. A. & Kjelleberg, S. 2016 Biofilms: an emergent form of bacterial life. *Nat. Rev. Microbiol.* **14**, 563.

Hiraishi, A., Yanase, A. & Kitamura, H. 1991 Polyphosphate accumulation by *Rhodobacter sphaeroides* grown under different environmental conditions with special emphasis on the effect of external phosphate concentrations. *Bull. Jpn. Soc. Microb. Ecol.* **6**, 25–32.

Law, Y., Kirkegaard, R. H., Cokro, A. A., Liu, X., Arumugam, K., Xie, C., Stokholm-Bjerregaard, M., Drautz-Moses, D., Nielsen, P. H., Wuertz, S. & Williams, R. B. H. 2016 Integrative microbial community analysis reveals full-scale enhanced biological phosphorus removal under tropical conditions. *Sci. Rep.* **6** (1), 25719.

Majed, N. & Gu, A. Z. 2019 Impact of influent carbon to phosphorus ratio on performance and phenotypic dynamics in enhanced biological phosphorus removal (EBPR) system-insights into carbon distribution, intracellular polymer stoichiometry and pathways shifts. bioRxiv:671081.

Marques, R., Santos, J., Nguyen, H., Carvalho, G., Noronha, J. P., Nielsen, P. H., Reis, M. A. M. & Oehmen, A. 2017 Metabolism and ecological niche of *Tetrasphaera* and *Ca*. Accumulibacter in enhanced biological phosphorus removal. *Water Res.* **122**, 159–171.

McIlroy, S. J., Kirkegaard, R. H., McIlroy, B., Nierychlo, M., Kristensen, J. M., Karst, S. M., Albertsen, M. & Nielsen, P. H. 2017 MiDAS 2.0: an ecosystem-specific taxonomy and online database for the organisms of wastewater treatment systems expanded for anaerobic digester groups. *Database (Oxford)* **2017**, 1–9.

Nadell, C. D., Drescher, K. & Foster, K. R. 2016 Spatial structure, cooperation and competition in biofilms. *Nat. Rev. Microbiol.* **14**, 589–600.

Quast, C., Pruesse, E., Yilmaz, P., Gerken, J., Schweer, T., Yarza, P., Peplies, J. & Glockner, F. O. 2013 The SILVA ribosomal RNA gene database project: improved data processing and web-based tools. *Nucleic Acids Res.* **41**, D590–D596.

Rotem, O., Pasternak, Z., Jurkevitch, E., 2014 *Bdellovibrio* and like organisms. In: *The Prokaryotes: Deltaproteobacteria and Epsilonproteobacteria* (Rosenberg, E., DeLong, E. F., Lory, S., Stackebrandt, E. & Thompson, F., eds). Springer Berlin Heidelberg, Berlin, Heidelberg, pp. 3–17. doi:10.1007/978-3-642-39044-9_379.

Rudi, K., Goa, I. A., Saltnes, T., Sorensen, G., Angell, I. L. & Eikas, S. 2019 Microbial ecological processes in MBBR biofilms for biological phosphorus removal from wastewater. *Water Sci. Technol.* **79**, 1467–1473.

Saltnes, T., Sorensen, G. & Eikas, S. 2017 Biological nutrient removal in a continuous biofilm process. *Water Pract. Technol.* **12**, 797–805.

Sauer, K., Stoodley, P., Goeres, D. M., Hall-Stoodley, L., Burmølle, M., Stewart, P. S. & Bjarnsholt, T. 2022 The biofilm life cycle: expanding the conceptual model of biofilm formation. *Nat. Rev. Microbiol.* doi:10.1038/s41579-022-00767-0.

Suarez, C., Persson, F. & Hermansson, M. 2015 Predation of nitritation–anammox biofilms used for nitrogen removal from wastewater. *FEMS Microbiol. Ecol.* **91**, 1–9.

Sun, Y., Peng, Y., Chen, Y., Zhang, Q. & Li, X. 2022 Insights into the denitrifying phosphorus removal decay processes by profiling of the response mechanism of denitrifying phosphate-accumulating organisms to starvation stress. *Bioresour. Technol.* **357**, 127352.

Vargas, M., Yuan, Z. & Pijuan, M. 2013 Effect of long-term starvation conditions on polyphosphate- and glycogen-accumulating organisms. *Bioresour. Technol.* **127**, 126–131.

Villard, D., Saltnes, T., Sorensen, G., Angell, I. L., Eikas, S., Johansen, W. & Rudi, K. 2022 Spatial fractionation of phosphorus accumulating biofilm: stratification of polyphosphate accumulation and dissimilatory nitrogen metabolism. *Biofouling* **38**, 162–172.

Wang, L., Yan, J., Wise, M. J., Liu, Q., Asenso, J., Huang, Y., Dai, S., Liu, Z., Du, Y. & Tang, D. 2018 Distribution patterns of polyphosphate metabolism pathway and its relationships with bacterial durability and virulence. *Front. Microbiol.* **9**, 782–782.